SANDIA REPORT

SAND97–2629 • UC–705
Unlimited Release
Printed October 1997

An Algorithm for Enforcement of Contact Constraints in Quasistatic Applications Using Matrix-free Solution Algorithms

M. W. Heinstein

Prepared by
Sandia National Laboratories
Albuquerque, New Mexico 87185 and Livermore, California 94550

Sandia is a multiprogram laboratory operated by Sandia Corporation, a Lockheed Martin Company, for the United States Department of Energy under Contract DE-AC04-94AL85000.

Issued by Sandia National Laboratories, operated for the United States Department of Energy by Sandia Corporation.

Available to DOE and DOE contractors from
Office of Scientific and Technical Information
P.O. Box 62
Oak Ridge, TN 37831

Prices available from (615) 576-8401, FTS 626-8401

Available to the public from
National Technical Information Service
U.S. Department of Commerce
5285 Port Royal Rd
Springfield, VA 22161

NTIS price codes
Printed copy: A03
Microfiche copy: A01

SAND97-2629
Unlimited Release
Printed October 1997

Distribution
Category UC-705

An Algorithm for Enforcement of Contact Constraints in Quasistatic Applications using Matrix-free Solution Algorithms

M.W. Heinstein
Engineering Mechanics and Material Modeling Department
Sandia National Laboratories
P.O. Box 5800
Albuquerque, New Mexico 87185-0443

Abstract

A contact enforcement algorithm has been developed for matrix-free quasistatic finite element techniques. Matrix-free (iterative) solution algorithms such as nonlinear Conjugate Gradients (CG) and Dynamic Relaxation (DR) are distinctive in that the number of iterations required for convergence is typically of the same order as the number of degrees of freedom of the model. From iteration to iteration the contact normal and tangential forces vary significantly making contact constraint satisfaction tenuous. Furthermore, global determination and enforcement of the contact constraints every iteration could be questioned on the grounds of efficiency. This work addresses this situation by introducing an intermediate iteration for treating the active gap constraint and at the same time exactly (kinematically) enforcing the linearized gap *rate* constraint for both frictionless and frictional response.

Nomenclature

$\varphi^{(i)}$	motion of body i
$\Omega^{(i)}$	local reference configuration of body i
$\Gamma^{(i)}$	surface of body i on which contact is expected
$\partial\Omega^{(i)}$	surface of body i
X	material point (location) on body 1
Y	material point (location) on body 2
t	time
$g(X, t)$	gap function
ν	outward normal vector
$\mathbf{t}$	Piola traction
t_N	contact pressure (normal traction)
t_T	contact tangential traction
$g_N(X, t)$	normal gap
$g_T(X, t)$	tangential gap
$\dot{g}_N$	normal gap rate
$\dot{g}_T$	tangential gap rate
μ	Coulomb friction coefficient
$V^{(i)}(X)$	instantaneous material volocity at X
$\overset{*}{\varphi}$	admissible material variation of body's motion
$H\left(\overset{*}{\varphi}, \varphi\right)$	sum of internal and external virtual work
$H_c\left(\overset{*}{\varphi}, \varphi\right)$	contact virtual work
$d(t)$	unknown solution vector i.e. the discrete form of φ
F^{int}	internal force vector due to the stress divergence
F_c	contact force vector
F^{ext}	applied force vector
$\Delta d(t)$	unknown incremental solution vector
υ^i	unit normal at node i
g_N^i	discrete normal gap
g_T^i	discrete tangential gap at node i

G_N^i	transformation matrix from $\Delta d(t)$ to the discrete normal gap at node i
G_T^i	transformation matrix from $\Delta d(t)$ to the discrete tangential gap at node i
n_{con}	number of discrete constraints
$r_j(\Delta d_j(t))$	residual vector
s_j	conjugate gradient search direction for iteration j
M^{-1}	conjugate gradient diagonal preconditioner
β_j	conjugate gradient Gramm Schmidt constant
α_j	conjugate gradient line search parameter
ε	residual force convergence tolerance
ε_N^d	gap penalty
ε_N^v	gap rate penalty

Table of Contents

List of Tables

List of Figures

1 Introduction

Finite element implementations of contact problems have appeared frequently in the literature, (e.g. [1-4]), and have traditionally emphasized problems amenable to quasistatic and implicit dynamic frameworks using direct (matrix) solution methods. In such treatments it is typical to define a contact constraint wherein the contact force is conjugate to the approach, or gap, between opposing surfaces. Among the most recent methods applied to enforce the contact constraints is the method of Augmented Lagrangians (e.g. [5,7]) which is able to circumvent ill-conditioning while still providing accurate constraint enforcement.

The distinctive nature of an iterative (matrix-free) solution methodology, on the other hand, motivates this investigation. Although several contact treatments have been presented for explicit transient dynamic applications (e.g. [8,9]) the focus here is on explicit quasi-static applications. Algorithms such as nonlinear Conjugate Gradients and Dynamic Relaxation are examples of explicit iterative solvers. They typically require a significant number of iterations for convergence particularly for nonlinear applications. In this setting, the contact normal and tangential forces vary dramatically from iteration to iteration making constraint satisfaction tenuous. Furthermore, although global determination and enforcement of the contact constraints every iteration has been demonstrated in SANTOS [10] and JAC3D [11], the efficiency of this approach could be questioned. This work addresses these shortcomings by introducing an intermediate iteration for treating the active gap constraint and at the same time exactly (kinematically) enforcing the linearized gap *rate* constraint for both frictionless and frictional response.

The application of the proposed algorithm is in JAS3D [12] a general purpose code developed at Sandia National Labs for the solution of nonlinear solid mechanics problems. It has both a nonlinear Conjugate Gradient and a nonlinear Dynamic Relaxation solver. In the work that is presented here, the focus is on the nonlinear Conjugate Gradients solver, with application to Dynamic Relaxation being straightforward.

Section 2 presents the formulation of the general contact problem with specialization to Quasistatics in Section 3. Following a summary of the Conjugate Gradient algorithm in JAS3D, a detailed description of the choices for contact constraint enforcement is given in Section 4 including the presentation of the proposed algorithm. Finally, Section 5 presents example problems that demonstrate the effectiveness of the proposed algorithm.

2 Problem Formulation

Contact constraint definition

Consider the motions $\varphi^{(1)}$ and $\varphi^{(2)}$ of two deformable bodies, denoted in their reference configurations by $\Omega^{(1)}$ and $\Omega^{(2)}$, and select $\Gamma^{(1)} \subset \partial\Omega^{(1)}$ and $\Gamma^{(2)} \subset \partial\Omega^{(2)}$ to include all prospective contact points over the time interval [0,T]. Choosing any material point $X \in \Gamma^{(1)}$, the gap function g is defined with respect to $\Gamma^{(2)}$ as:

$$g(X, t) = \min_{Y \in \Gamma^{(2)}} \left\| \varphi^{(1)}(X) - \varphi^{(2)}(Y) \right\| \text{sign}(g) \tag{1}$$

where

$$\text{sign}(g) = \begin{cases} -1 \text{ if } \varphi^{(1)}(X) \text{ lies in the interior of } \varphi^{(2)}(\Omega^{(2)}), \\ 1 \text{ otherwise} \end{cases} \tag{2}$$

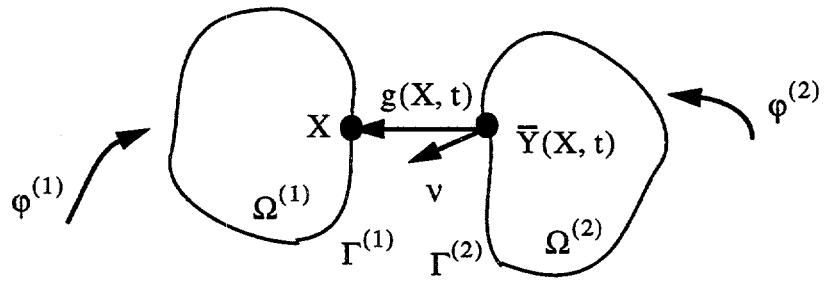

Figure 1. Motion of two bodies and definition of the contact gap

The material point of $\Gamma^{(2)}$ satisfying the minimization of (1) is denoted as $\bar{Y}(X, t)$, as shown in Figure 1. The contact pressure acting on the point X is written as

$$t_N = -t\nu \quad \text{(positive if compressive)} \tag{3}$$

and the contact tangential traction acting on the point X as

$$t_T = -t(1 - \nu) \tag{4}$$

where t is Piola traction acting at X and ν is the outward normal at $\varphi^{(2)}(\bar{Y}(X, t))$. Further, the normal and tangential gaps are written as:

$$\begin{aligned} g_N(X, t) &= \nu \bullet g(X, t) \\ g_T(X, t) &= (1 - \nu) \bullet g(X, t) \end{aligned} \tag{5}$$

With these notations, the contact constraints to be enforced for all $X \in \Gamma^{(1)}$ and for all $t \in [0,T]$ are summarized for frictionless response as:

$$\begin{cases} g_N \geq 0 \\ t_N \geq 0 \\ t_N g_N = 0 \\ t_N \dot{g}_N = 0 \end{cases} \tag{6}$$

Graphically, these normal contact constraints are shown in Figure 2.

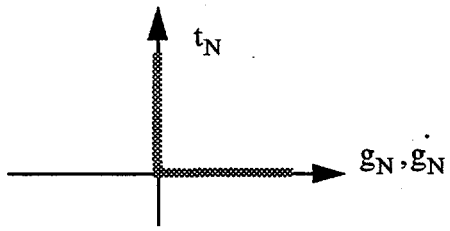

Figure 2. Graphical representation of normal contact constraints

The additional contact constraints required for frictional response are:

$$\begin{cases} \begin{pmatrix} t_T g_T = 0 \\ t_T \dot{g}_T = 0 \end{pmatrix} & \text{if } |t_T| \leq \mu t_N \\ t_T g_T \geq 0 & \text{if } |t_T| = \mu t_N \end{cases} \tag{7}$$

which are shown graphically in Figure 3.

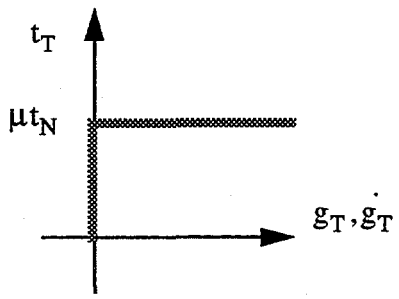

Figure 3. Graphical representation of tangential (frictional) contact constraints

Notably, the persistency condition, i.e. $t_N \dot{g}_N = 0$ in $(6)_4$ and $t_T \dot{g}_T = 0$ in $(7)_2$ is ordinarily not used in traditional direct solution implementations but becomes particularly useful for matrix-free iterative solution techniques. Finally, it is noted that the material time derivative of the gap functions can be evaluated without approximation as:

$$\begin{aligned} \dot{g}_N &= \nu \bullet (V^{(1)}(X) - V^{(2)}(\bar{Y})) \\ \dot{g}_T &= (I - \nu) \bullet (V^{(1)}(X) - V^{(2)}(\bar{Y})) \end{aligned} \tag{8}$$

where $V^{(1)}(X)$ and $V^{(2)}(\bar{Y})$ are the instantaneous material velocities of X and $\bar{Y}$, respectively. Linearity of both $\dot{g}_N$ and $\dot{g}_T$ in the respective material velocities is useful computationally as will be seen later.

Variational principle

Integrating the weighted local momentum balance in each body and combining, one can show that the following variational principle holds for the two body system (see e.g. [6]):

$$H\left(\overset{*}{\varphi}, \varphi\right) + H_c\left(\overset{*}{\varphi}, \varphi\right) = 0 \tag{9}$$

where φ is the collection of the $\varphi^{(i)}$ and $\overset{*}{\varphi}$ is an admissible material variation. $H\left(\overset{*}{\varphi}, \varphi\right)$ is the sum of the inertial virtual work and the virtual work of the specified boundary tractions and body forces, and includes contributions from both bodies. $H_c\left(\overset{*}{\varphi}, \varphi\right)$ is the contact virtual work, which has the following form (with a contribution from both normal and frictional response):

$$H_c\left(\overset{*}{\varphi}, \varphi\right) = \int_{\Gamma^{(1)}} (t_N \delta g_N + t_T \delta g_T) d\Gamma^{(1)} \tag{10}$$

where δg_N and δg_T are the directional derivatives of g_N and g_T in the direction of $\overset{*}{\varphi}$, i.e.:

$$\begin{cases} \delta g_N := \dfrac{d}{d\alpha}\Big|_{\alpha = 0} \left[g_N\left(\varphi + \alpha \overset{*}{\varphi}\right) \right] \\ \qquad\qquad \text{and} \\ \delta g_T := \dfrac{d}{d\alpha}\Big|_{\alpha = 0} \left[g_T\left(\varphi + \alpha \overset{*}{\varphi}\right) \right] \end{cases} \tag{11}$$

It is noted that t_N and t_T in (10) are subject to constraints (6) and (7), respectively.

3 Numerical Implementation: Quasistatics

Application of the finite element method to the variational principle summarized by (9) gives rise to the following set of nonlinear equations:

$$F^{int}(d(t)) + F_c(d(t)) = F^{ext}(t) \tag{12}$$

which holds for all $t \in [0,T]$. In equation (12) the inertial force term has been omitted (quasistatic assumption) but t still serves as the load step indication, $d(t)$ is the unknown solution vector i.e. the discrete form of φ, F^{int} is the internal force vector due to the stress divergence, F_c is the contact force vector, and F^{ext} is the applied force vector. Typically, nonlinear problems will require load steps, in which case (12) becomes

$$F^{int}(d(t-\Delta t) + \Delta d(t)) + F_c(d(t-\Delta t) + \Delta d(t)) = F^{ext}(t) \tag{13}$$

where now $d(t-\Delta t)$ is the known solution and $\Delta d(t)$ is the unknown incremental solution.

Because of the temporal and spatial discretization, the contact constraints are assumed to apply to nodes on one surface and finite element faces on the other at specific times during the solution. In this case, the discrete forms of the gap functions are:

$$\begin{aligned} g_N^i &= \upsilon^i \bullet (\Delta d^i(t) - \Delta d_c{}^i(t)) \\ g_T^i &= (1-\upsilon^i) \bullet (\Delta d^i(t) - \Delta d_c{}^i(t)) \end{aligned} \tag{14}$$

where i denotes a particular surface node (called a slave node) with incremental motion $\Delta d^i(t)$, which is contacting a point on the opposing surface with incremental motion $\Delta d_c{}^i(t)$. Almost always this point requires interpolation of the nodal quantities defining the discrete representation of the surface (called a master surface).

It will be convenient, then, to write equation (14) as:

$$\begin{aligned} g_N^i &= G_N^i \Delta d(t) \\ g_T^i &= G_T^i \Delta d(t) \end{aligned} \tag{15}$$

where G_N^i and G_T^i include the interpolation, differences and orientation required (when multiplied by $\Delta d(t)$) to provide the discrete gap at node i. Combining all G_N^i and G_T^i gives:

$$\begin{aligned} g_N &= G_N \Delta d(t) \\ g_T &= G_T \Delta d(t) \end{aligned} \tag{16}$$

which are the normal and tangential n_{con}-vectors of the discrete constraints.

At this point the iterative solution methodology can be considered. Although a description of the Conjugate Gradient (CG) algorithm is given here, it is not intended to be a review of the theory. A well presented review of the theory and concepts behind linear CG can be found in [13]. Also in [13] is some discussion of nonlinear CG including other references on the subject.

Conjugate Gradient Iterative solution

The CG algorithm of interest, Preconditioned Nonlinear Conjugate Gradients with Secant Method and Polak-Ribiere, can be summarized as follows (further details can be found in JAC3D [11] and JAS3D [12]) :

introduce the CG iteration counter j, and for $j = 0, \max \text{ iterations}$

Compute the residual,

$$r_j(\Delta d_j(t)) = F^{ext}(t) - [F^{int}(d(t-\Delta t) + \Delta d_j(t)) + F_c(d(t-\Delta t) + \Delta d_j(t))]$$

Compute the conjugate search direction,

$$s_{j+1} = M^{-1} r_j + \beta_j s_j$$

where M is the Jacobi diagonal preconditioner and the Gramm Schmidt constant is based on the Polak-Ribiere formula:

$$\beta_j = \begin{cases} \max\left(\dfrac{r_j^T M^{-1}(r_j - r_{j-1})}{r_{j-1}^T M^{-1} r_{j-1}}, 0 \right) & j > 0 \\ 0 & j = 0 \end{cases}$$

Compute the incremental displacement,

$$\Delta d_{j+1} = \Delta d_j + \alpha_j s_{j+1}$$

where the line search parameter minimizes the residual along the search direction using the Secant Method:

$$\alpha_j = \frac{r_j^T s_j}{r_j^T (\Delta d_j + s_{j+1}) s_j - r_j^T s_j}$$

Convergence is obtained when $r_j(\Delta d_j(t)) \le \varepsilon$, and $\Delta d_j(t)$ is the desired solution.

4 Choices for Constraint Enforcement

The basic issue in constraint implementation is whether to directly enforce the gap constraint $t_N g_N = 0$ (equation $(6)_3$), the gap rate constraint i.e. the persistency condition $t_N \dot{g}_N = 0$ (equation $(6)_4$), or some weighted average of both. Use of the displacement penalty parameter and/or the velocity penalty to enforce $(6)_3$ and $(6)_4$ has been explored by [9] and can be achieved in the current iterative scheme by expressing F_c via:

$$F_c(d(t-\Delta t)+\Delta d_j(t)) = \varepsilon_N^d G_N{}^T G_N \Delta d_j(t) + \varepsilon_N^v G_N{}^T G_N s_{j+1} \qquad (17)$$

which is the sum of a gap penalization (using ε_N^d) and a gap rate penalization (using ε_N^v). Recall that G_N is an $n_{con} \times n_{eq}$ matrix, generally depending on the deformation, which multiplies $\Delta d_j(t)$ and s_{j+1} to produce an n_{con} - vector of the discrete normal constraints, see equation (16). For notational simplicity, this vector is assumed to contain zero entries for those constraints which are not currently active. The vector is then penalized to obtain normal contact forces. Note that the matrix G_N in (17) is the same for both kinematic constraints; this is a direct consequence of equation (8).

Algorithm 1 summarizes CG with displacement penalty only, where it is seen that the constraints at the known iterate j are penalized. As noted in [4], this makes the Lagrange multipliers singular.

Algorithm 1: CG with displacement penalty - frictionless

$$r_j(\Delta d_j(t)) = F^{ext}(t) - [F^{int}(d(t-\Delta t)+\Delta d_j(t)) + \varepsilon_N^d G_N{}^T G_N \Delta d_j(t)]$$

$$s_{j+1} = M^{-1} r_j + \beta_j s_j$$

$$\Delta d_{j+1} = \Delta d_j + \alpha_j s_{j+1}$$

Experience shows this the case to be as well, i.e. the displacement penalty method by itself is ill-conditioned when seeking accurate contact enforcement and is particularly true in the CG iterative framework. A stiff penalization combined with the line search $(Alg.\ 1)_3$ consistently overpredicts the contact force resulting in loss of contact. Yet, a soft penalization that underpredicts the contact force combined with the conjugacy of the CG search directions $(Alg.\ 1)_2$ will be extremely slow to converge. Handling of the tangential constraint is even more difficult since neither t_N or t_T in equation $(7)_1$ is well defined during the CG iterations. For the moment, without further numerical treatment, the gap constraints will remain difficult to satisfy. The proper treatment of the rate constraints, however, will lay the necessary foundation for their eventual treatment.

Gap Rate Constraints - Normal Constraint

The rate constraint can be effectively implemented with some numerical approximation. To show this, the CG algorithm with velocity penalty is written in a Langrange multiplier form as *Algorithm 2*.

Algorithm 2: CG with velocity penalty - frictionless

$$r_j(\Delta d_j(t)) = F^{ext}(t) - [F^{int}(d(t-\Delta t) + \Delta d_j(t)) + G_N^T \lambda_j^{nor}]$$

$$s_{j+1} = M^{-1} r_j + \beta_j s_j$$

$$\Delta d_{j+1} = \Delta d_j + \alpha_j s_{j+1}$$

$$G_N s_{j+1} = 0$$

Solving *Algorithm 2* for λ_j^{nor} yields:

$$G_N M^{-1} G_N^T \lambda_j^{nor} - G_N \beta_j s_j = F^{ext} - F_j^{int} \tag{18}$$

where the simplified notation $F_j^{int} = F^{int}(d(t-\Delta t) + \Delta d_j(t))$ and $F^{ext} = F^{ext}(t)$ has been adopted. The coefficient matrix $[G_N M^{-1} G_N^T]$ on the left hand side of (18) is not in general diagonal. This is troublesome in practice, yet the real difficulty with (18) stems from the Gramm Schmidt constant's dependence on the Lagrange multipliers, i.e.:

$$\begin{aligned} \beta_j &= \frac{r_j^T (r_j - r_{j-1})}{r_{j-1}^T r_{j-1}} \\ &= \frac{-[F^{ext} - F_j^{int} - G_N^T \lambda_j^{nor}]^T [(F_j^{int} - F_{j-1}^{int}) + (G_N^T \lambda_j^{nor} - G_N^T \lambda_{j-1}^{nor})]}{[F^{ext} - F_{j-1}^{int} - G_N^T \lambda_{j-1}^{nor}]^T [F^{ext} - F_{j-1}^{int} - G_N^T \lambda_{j-1}^{nor}]} \end{aligned} \tag{19}$$

where it is now evident that (18) also contains a polynomial in the Lagrange multipliers λ_j^{nor}. Practically, this makes (18) unsolvable in the iterative setting since the solution of the tightly coupled system would be prohibitive every CG iteration.

Numerical approximation to *Algorithm 2* is possible with a specialization of the rate constraint to one-sided contact (so called master-slave contact) such that the difficulty of directly solving equation (18) is addressed.

Specialization to one-sided contact

Specialization of *Algorithm 2* to one-sided contact is made by writing the rate constraint $(Alg.\ 2)_4$ with its slave and master contributions:

$$G_N s_{j+1} = G_N^s s_{j+1} + G_N^m s_{j+1} = 0 \tag{20}$$

and assuming a solution to $(Alg.\ 2)_1$ as:

$$0 = G_N^s r_j = G_N^s (F^{ext} - F_j^{int} - G_N^T (\lambda_j^{nor})_{trial}) \tag{21}$$

Combining (20) and (21), one can show that

$$G_N^s (F^{ext} - F_j^{int}) = G_N^s (G_N^s)^T (\lambda_j^{nor})_{trial} = (\lambda_j^{nor})_{trial} \tag{22}$$

where taken advantage of in (22) are the useful properties of G_N^s and G_N^m :

$$G_N^s (G_N^m)^T = \underset{n_{con} \times n_{con}}{0} \tag{23}$$

and

$$G_N^s (G_N^s)^T = \underset{n_{con} \times n_{con}}{1} \tag{24}$$

Interestingly, a physical interpretation of (22) is seen in Figure 4:

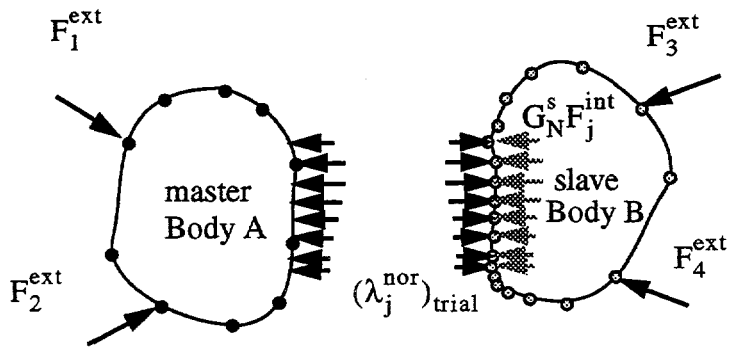

Figure 4. Physical interpretation of the Lagrange multipliers $(\lambda_j^{nor})_{trial}$

where is seen that only one side of the contact is considered (namely those constraints defined on Body B). The trial solution for the contact forces $(\lambda_j^{nor})_{trial}$ are a direct result of the stress divergence at the contact surface nodes of the slave Body B *alone*.

Substituting result (22) into $(Alg.\ 2)_1$, the residual at the j^{th} CG iteration can be computed as:

$$\begin{aligned} r_j(\Delta d_j(t)) &= F^{ext} - F_j^{int} - (G_N)^T G_N^s (F^{ext} - F_j^{int}) \\ &= \left[\underset{n_{eq} \times n_{eq}}{1} - (G_N)^T G_N^s \right] (F^{ext} - F_j^{int}) \end{aligned} \tag{25}$$

Because of assumption (21), the search direction must now be augmented to include slave node contributions, i.e.:

$$s_{j+1} = (M^{-1} r_j + \beta_j s_j) + s^s{}_{j+1} \tag{26}$$

where $s^s{}_{j+1}$ is found using the kinematic constraint, equation (20):

$$s^s{}_{j+1} = -(G_N^s)^T G_N^m (M^{-1} r_j + \beta_j s_j) \tag{27}$$

Note that the slave node degrees of freedom are now explicitly determined, and the resulting algorithm is no longer a penalty method. Summarizing, the CG algorithm with frictionless velocity constraint (*Alg. 3*) is written as:

Algorithm 3: CG with kinematic velocity constraint and one-sided contact - frictionless

$$r_j(\Delta d_j(t)) = \left[\underset{n_{eq} \times n_{eq}}{1} - (G_N)^T G_N^s \right] (F^{ext}(t) - F^{int}(d(t - \Delta t) + \Delta d_j(t)))$$

$$s_{j+1} = \left[\underset{n_{eq} \times n_{eq}}{1} - (G_N^s)^T G_N^m \right] (M^{-1} r_j + \beta_j s_j)$$

$$\Delta d_{j+1} = \Delta d_j + \alpha_j s_{j+1}$$

Gap Rate Constraints - Tangential Constraint

The tangential rate constraint is applied analogously to the normal rate constraint, i.e. assuming a sticking condition $(Alg.\ 2)_1$ is written as:

$$r_j = F^{ext} - (F_j^{int} + G_N^T \lambda_j^{nor} + G_T^T (\lambda_j^{tan})_{stick}) \tag{28}$$

And again making the one-sided contact assumption, equation (28) is written as:

$$0 = G_T^s r_j = G_T^s [F^{ext} - (F_j^{int} + G_N^T \lambda_j^{nor} + G_T^T (\lambda_j^{tan})_{stick})] \tag{29}$$

from which $(\lambda_j^{tan})_{stick}$ can be found as:

$$G_T^s(F^{ext} - F_j^{int}) - G_T^s G_N^T \lambda_j^{nor} = G_T^s (G_T^s)^T (\lambda_j^{tan})_{stick} = (\lambda_j^{tan})_{stick} \tag{30}$$

The stick - slip discontinuity in the contact force can now be considered:

$$\lambda_j^{tan} = \begin{cases} (\lambda_j^{tan})_{stick} & \text{if } (\lambda_j^{tan})_{stick} \le \mu \lambda_j^{nor} \\ (\lambda_j^{tan})_{slip} = \mu \lambda_j^{nor} & \text{if } (\lambda_j^{tan})_{stick} > \mu \lambda_j^{nor} \end{cases} \tag{31}$$

where Coulomb friction is assumed to hold. Finally, the search direction must be modified for sticking conditions:

$$s_{j+1}^{stick} = \begin{cases} -(G_T^s)^T G_T^m (M^{-1} r_j + \beta_j s_j) & \text{if sticking} \\ 0 & \text{otherwise} \end{cases} \tag{32}$$

Summarizing, the CG algorithm with kinematic velocity constraint and one-sided contact (*Alg. 4*) is written as:

Algorithm 4: CG with kinematic velocity constraint and one-sided contact - general

$$r_j(\Delta d_j(t)) = \left[\underset{n_{eq} \times n_{cq}}{1} -(G_N)^T G_N^s \right](F^{ext} - F_j^{int}) - (G_T)^T \lambda_j^{tan}$$

$$\lambda_j^{tan} = \min[G_T^s(F^{ext} - F_j^{int}), \mu G_N^s(F^{ext} - F_j^{int})]$$

$$s_{j+1} = \left[\underset{n_{eq} \times n_{eq}}{1} -(G_N^s)^T G_N^m \right](M^{-1} r_j + \beta_j s_j) + s_{j+1}^{stick}$$

$$s_{j+1}^{stick} = \begin{cases} -(G_T^s)^T G_T^m (M^{-1} r_j + \beta_j s_j) & \text{if sticking} \\ 0 & \text{otherwise} \end{cases}$$

$$\Delta d_{j+1} = \Delta d_j + \alpha_j s_{j+1}$$

Gap Constraints

Remaining now is the treatment of the normal and tangential gap constraint. Consideration of the displacement penalty during the CG iterative process was shown to be problematic because of its interaction with the CG methodology. Yet, with the gap rate constraint treatment (*Alg. 4*) as a foundation, the gap constraints can now be effectively considered.

Intermediate Iterations with Rate Constraint Linearization

It is proposed that the normal and tangential gap constraint be treated with the introduction of an intermediate iteration to (*Alg. 4*) - where the normal gaps are kinematically removed and some amount of frictional slip is allowed if required. This is accomplished in a loop around the CG algorithm and an incremental kinematic prescription of the gap removal, i.e.:

$$\Delta d_{k+1} = \Delta d_k + \Delta d_{j*} + \beta_N G_N^T G_N (d(t-\Delta t) + \Delta d_k + \Delta d_{j*}) \tag{33}$$

for the normal gap constraints. In equation (33), the second iteration counter k is the gap enforcement loop, Δd_k is the accumulated displacement increment for the k^{th} intermediate solution, Δd_{j*} is the displacement increment for the current $(k+1)^{th}$ intermediate solution, and β_N is a pushback factor, i.e. $0 < \beta_N \leq 1$ on the normal gap. A graphical depiction of this treatment is shown in Figure 5. It is seen that after a kinematic removal of a portion of the normal gap (horizontal lines), the rate constraints alone are active during the CG iterations (vertical lines); note that the CG algorithm converges at iteration $j = j^*$.

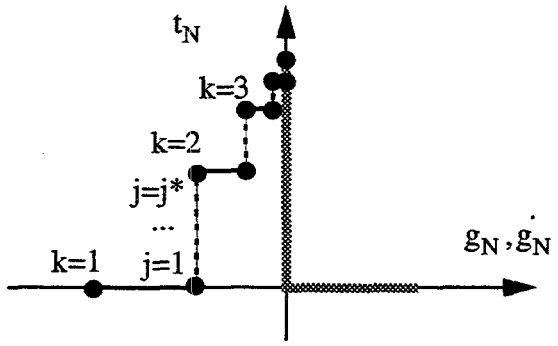

Figure 5. Incremental enforcement of normal gap constraint

The tangential gap constraints are treated in a similar manner, i.e.:

$$\Delta d_{k+1} = \Delta d_k + \Delta d_{j*} + \alpha M^{-1} (G_T^s)^T (\beta_T r_k^{tan}) \tag{34}$$

where α is the line search parameter, β_T is a allowable slip factor, i.e. $0 < \beta_T \leq 1$, and r_k^{tan} is the residual tangential force unbalance, i.e.

$$r_k^{tan} = \min[0, (G_T^s - \mu G_N^s)(F^{ext} - F_{j*}^{int})] \tag{35}$$

As shown in Figure 6, the tangential constraints are also gradually enforced. The frictional slip (horizontal lines) is determined from a line search along the steepest descent direction $M^{-1}(G_T^s)^T(\beta_T r_k^{tan})$, and the rate constraints are active during the CG iterations while assuming sticking conditions (vertical lines), i.e.

$$\lambda_j^{tan} = (\lambda_j^{tan})_{stick} = G_T^s(F^{ext} - F_j^{int}) \tag{36}$$

Importantly, equation (36) avoids the stick-slip decision during the CG iterations and allows the gap constraints (normal and tangential) to be enforced properly without interacting with the CG solution methodology.

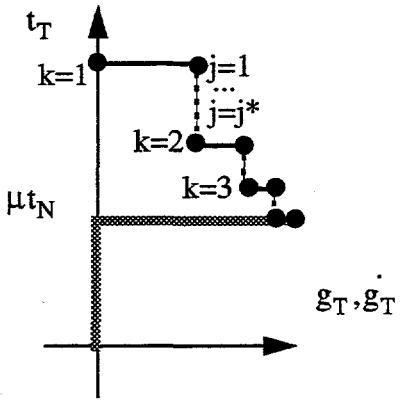

Figure 6. Incremental enforcement of the tangential gap constraint

The importance of this approximation can be understood by considering the behavior of the frictional constraint from iteration to iteration. It is seen in (*Alg. 4*) that a stick-slip decision is made based on the external forces and internal forces every iteration. However, the stress field is not yet in equilibrium and in some cases the external forces are still changing (i.e. in the case of an applied pressure). This can lead to errors in satisfying the frictional constraint since the slip is irrecoverable in a kinematic treatment.

Algorithmic Efficiency

This approach has an additional benefit via linearization of the active rate constraints. Rather than updating G_N^s and G_N^m (global degree-of-freedom to constraint transformations) every CG iteration j, they are held fixed until equilibrium. Recognizing that this is an intermediate equilibrium anyway (due to possible additional normal or tangential gap removal), $(G_N^s)_k$ and $(G_N^m)_k$ are updated (to $(G_N^s)_{k+1}$ and $(G_N^m)_{k+1}$) and another equilibrium configuration is sought. The updates k = 0, 1, 2, ... naturally converge when the residual after an update is below the user specified amount. The algorithm can be summarized in *Algorithm 5*.

Algorithm 5: CG with displacement penalty, kinematic velocity constraint and one-sided contact - general

introduce the gap constraint enforcement loop counter k, and for k = 0, 1, 2, ...

$$\Delta d_{k+1}(t) = \Delta d_k + (\Delta d_{j*})_k + \beta_N G_N^T G_N (d(t-\Delta t) + \Delta d_k + (\Delta d_{j*})_k)$$
$$+ \alpha M^{-1} (G_T^s)^T \beta_T \min[0, (G_T^s - \mu G_N^s)(F^{ext} - F^{int}(d(t-\Delta t) + \Delta d_k + (\Delta d_{j*})_k))]$$

where $\Delta d_{k=0} = 0$, and $(\Delta d_{j*})_k$ is determined by introducing the CG iteration counter j, and for j = 0, 1, 2, ...

Compute the residual, $r_j(\Delta d_j) = \left[\underset{n_{eq} \times n_{cq}}{1} - (G_N)^T G_N^s - (G_T)^T G_T^s \right] (F^{ext} - F_j^{int})$

Compute the conjugate search direction,

$$s_{j+1} = \left[\underset{n_{eq} \times n_{eq}}{1} - (G_N^s)^T G_N^m - (G_T^s)^T G_T^m \right] (M^{-1} r_j + \beta_j s_j)$$

where M is the diagonal preconditioner and the Gramm Schmidt constant is based on the Polak-Ribiere formula: $\beta_j = \max\left(\frac{r_j^T M^{-1} (r_j - r_{j-1})}{r_{j-1}^T M^{-1} r_{j-1}}, 0 \right)$ (with $\beta_0 = 0$)

Compute the incremental displacement, $\Delta d_{j+1} = \Delta d_j + \alpha_j s_{j+1}$

where the line search parameter minimizes the residual along the search direction using the Secant Method: $\alpha_j = \frac{r_j^T s_j}{r_j^T (\Delta d_j + s_{j+1}) s_j - r_j^T s_j}$

Convergence of the CG algorithm is obtained when $r_j((\Delta d_j(t))_k) \le \varepsilon$, and $(\Delta d_{j*}(t))_k = (\Delta d_j(t))_k$ is the desired solution.

Convergence of the gap enforcement loop is obtained when $r_{j=0}((\Delta d_0(t))_{k+1}) \le \varepsilon$ and $\Delta d_{k*} = \Delta d_k(t)$ is the desired solution.

5 Numerical Examples

Two examples are provided to demonstrate the important aspects of the proposed algorithm. Namely, that the extremely non-linear stick-slip frictional phenomenon can be robustly treated and that the efficiency of the contact constraint enforcement benefits from the constraint linearization.

Frictional Stick-Slip Example

The following problem is proposed by [14] and is solved here because of the analytical solution available (with small strain, one dimensional assumptions). As shown in Figure 7, it consists of a flat bar sliding against a rigid foundation. The loading is sequenced in the following manner. First, a vertical deflection of the top of the bar is prescribed such that the contact surface can support a tangential traction. Second, as a result of an applied load, p, the bar is gradually stretched causing progressive slipping along its length.

The bar has a length $L = 20$, a height $h = 2$, a thickness $t = 1$ and is meshed with 40 elements along its length, 4 thru its height and 4 thru its thickness. The elastic material is assumed to have the following properties: Youngs modulus E=10000 psi and poisson's ratio ν=0.0. Unless explicitly stated otherwise, the force convergence tolerance used in obtaining these results was ε=0.005.

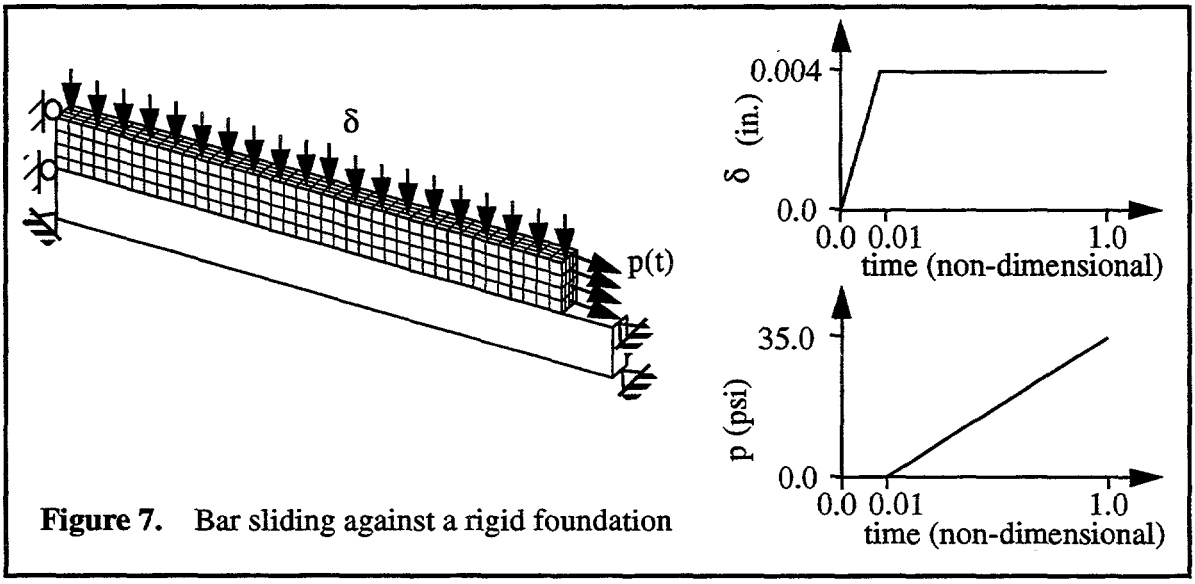

Figure 7. Bar sliding against a rigid foundation

The normal and tangential tractions for various times (several applied loads p) are shown in Figures 8 and 9 respectively. It is seen that the applied vertical deflection results in a nominal normal contact traction of 20 psi, although there is some two dimensional effect. The two dimensional effect is a result of the pressure "following" the non-planar deformation of the initial straight cross-section.

Notice that the tangential tractions are converged to that supported by the normal traction.

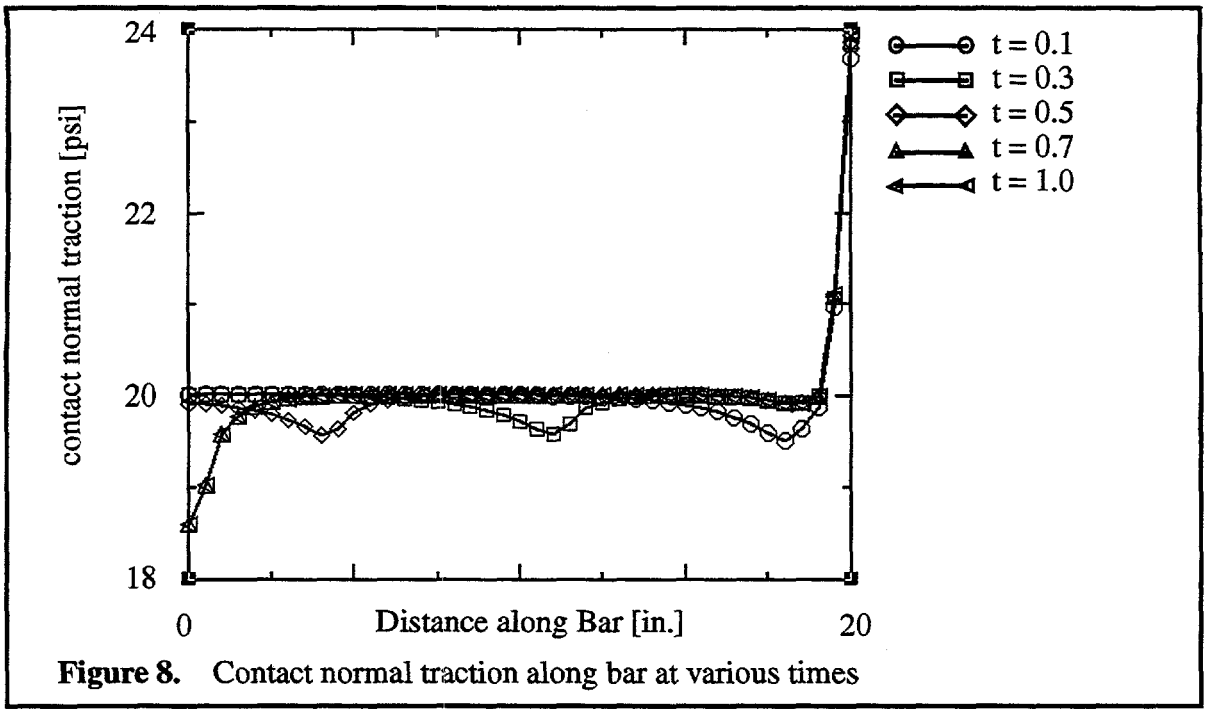

Figure 8. Contact normal traction along bar at various times

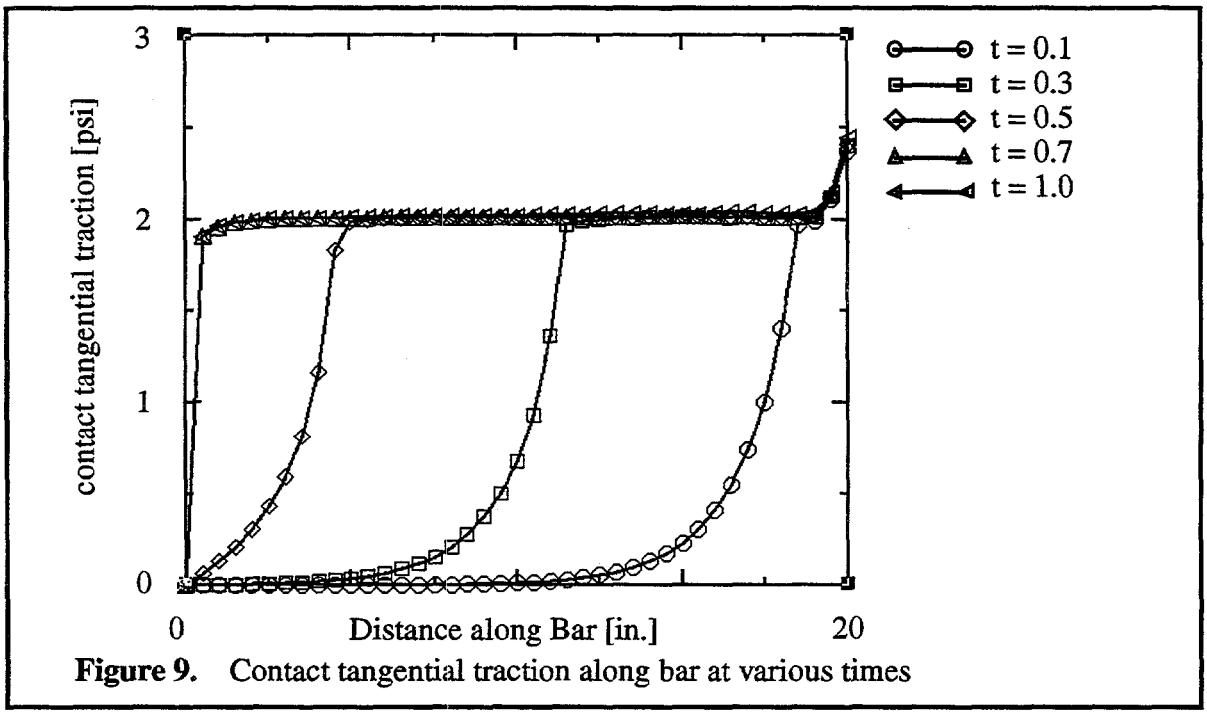

Figure 9. Contact tangential traction along bar at various times

Figure 10 is presented to indicate the quality of the constraint satisfaction that can be achieved. The frictional constraint satisfaction is shown to converge from "above" (that is to say it is always higher than that supported by the normal traction) as the convergence tolerance is progressively made smaller, in this case ε =0.05, 0.005, and 0.0005. This is a direct result of the slave node stiffness being higher than the stiffness corresponding to any of

the overall structural deformation modes. Thus, the amount of slip is determined based on the slave nodal stiffness M^{-1} ($\Delta slip = G_T^s \alpha M^{-1} (G_T^s)^T r_k^{tan}$) and is always conservatively predicted.

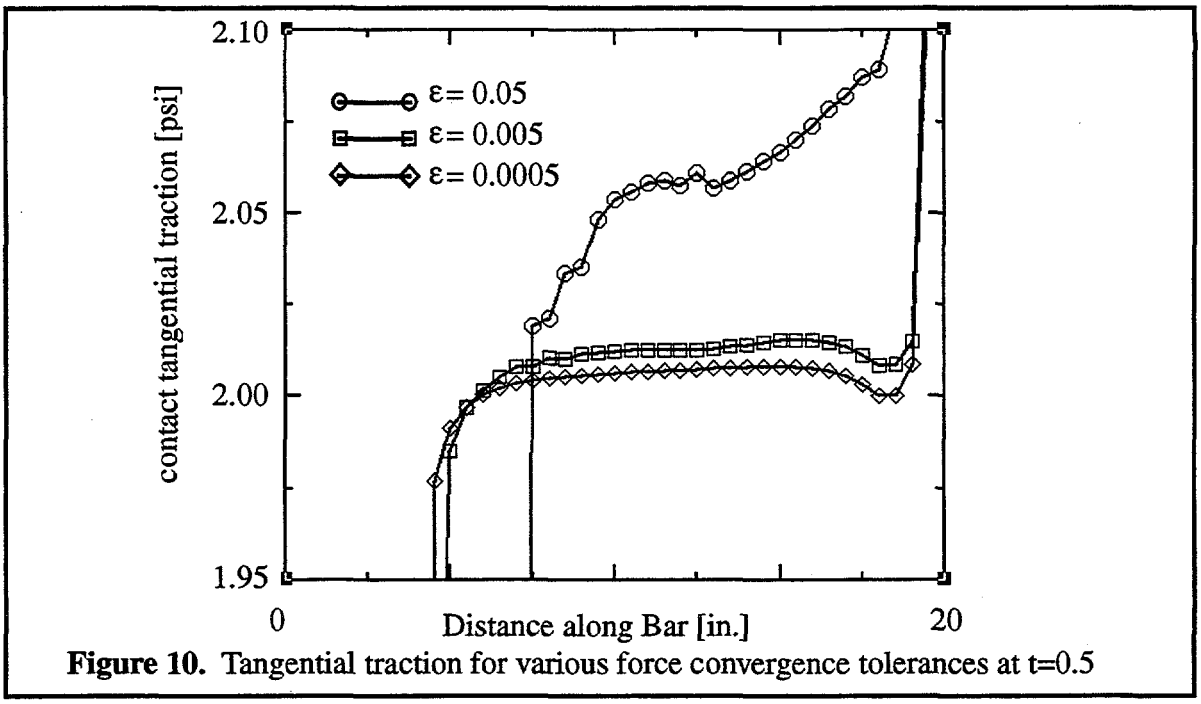

Figure 10. Tangential traction for various force convergence tolerances at t=0.5

Figure 11 shows the accumulated axial slip at the end of the bar as a function of time. The comparison between the analytical solution and the numerical solution appears acceptable.

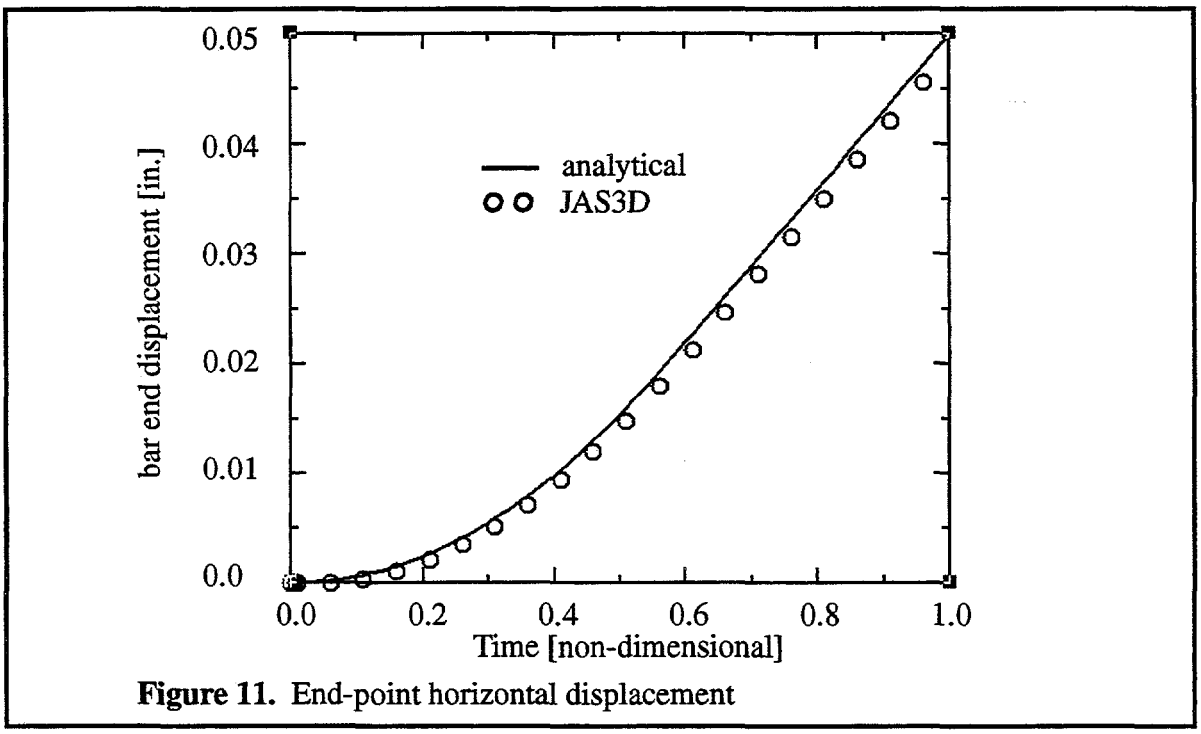

Figure 11. End-point horizontal displacement

A more precise comparison can be made by looking at the axial slip along the length of the bar. Figure 12 shows the accumulated axial slip at various times. It is seen that the proposed algorithm *(Alg. 5)* solves for the slip/no slip boundary (i.e. at time t=0.3 the slip/no slip boundary is located at approximately 12.5 in. along the length of the bar).

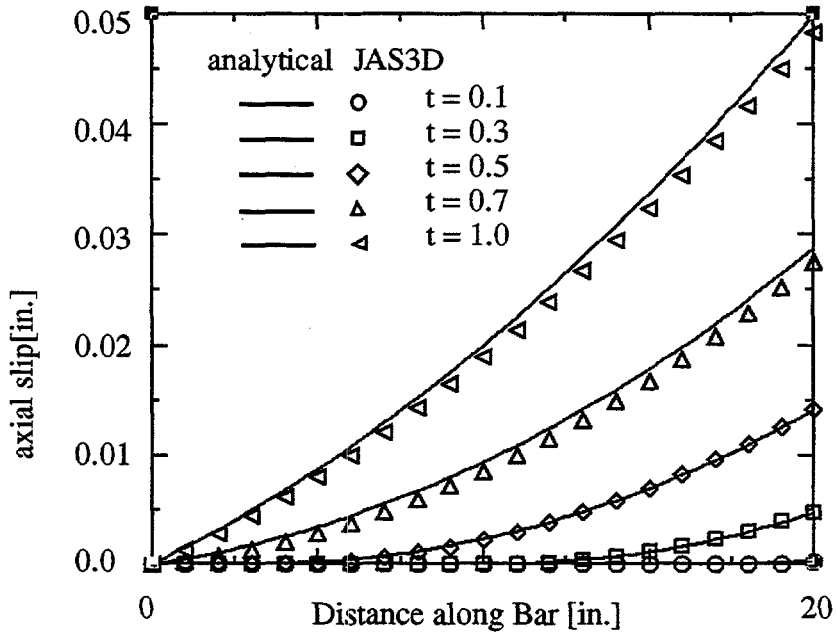

Figure 12. Accumulated axial slip along length of bar at various times

Example Problem with many Contacts

The following problem highlights the efficiency of linearizing the contact constraint definition. Figure 13 shows a symmetric model of an extrusion process. The Aluminum material is elastic-plastic with the following properties: Youngs modulus E = 68900 MPa, poisson's ratio $\nu = 0.3$, yield stress $\sigma_y = 68.9$ MPa, and Hardening Modulus H=0 MPa.

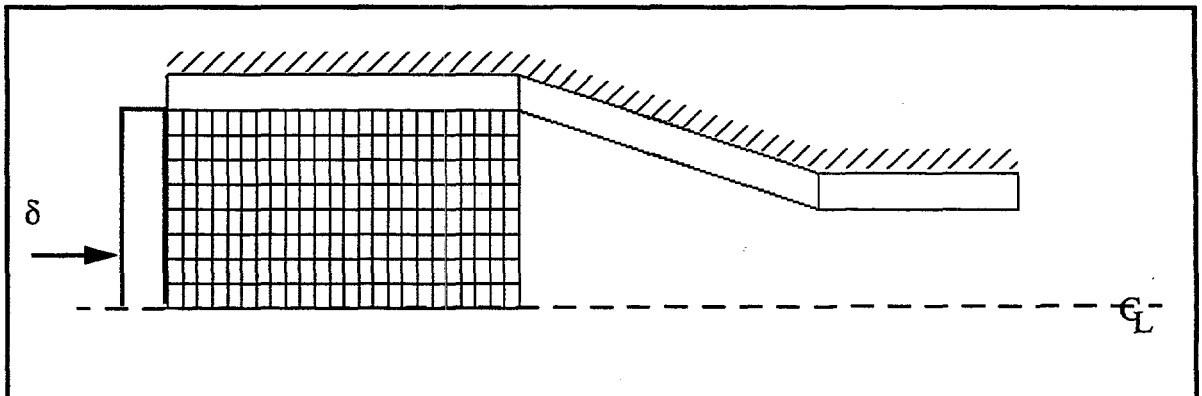

Figure 13. Symmetric half of an extrusion process

The force convergence tolerance was $\varepsilon = 0.005$ and both the CG and Dynamic Relaxation nonlinear iterative solution strategy was used. Figure 14 shows the typical deformed shape after prescribing a displacement $\delta = 0.038$m in 10 equal increments. The comparison made

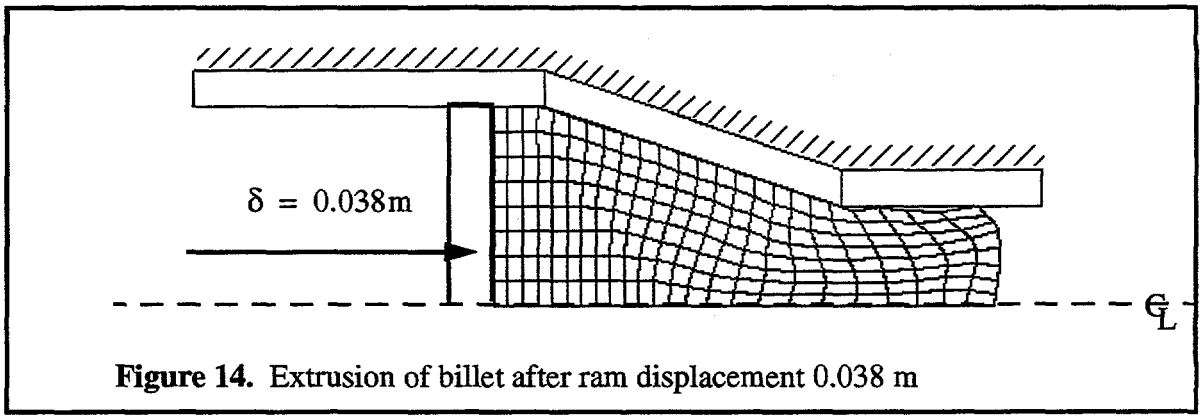

Figure 14. Extrusion of billet after ram displacement 0.038 m

here is between the CG (and DR) iterative solution using *Alg. 4* and *Alg. 5* (and DR counterpart to *Alg. 4* and *Alg. 5*, denoted as $(Alg.\ 4)_{DR}$ and $(Alg.\ 5)_{DR}$) for the contact constraint treatment. Table 1 summarizes the computational resources required (on a CRAY J90) for these simulations. It is seen that the linearized contact treatment (i.e. *Alg. 5*) using either CG or DR is considerably more efficient than not linearizing. Note also the added benefit of reducing the number of iterations for DR applications using $(\text{Alg. } 5)_{DR}$. This is due to a more optimal algorithmic damping that results from linearizing the contact constraints.

Table 1: Computational resources required for Extrusion simulation

Algorithm	Memory (Mb)	CPUs (J90)	iterations	CPUs/itr.
CG *Alg. 4*	2.243	445	12964	0.0343
CG *Alg. 5*	2.243	303	13810	0.0219
DR $(Alg.\ 4)_{DR}$	2.243	854	30911	0.0276
DR $(Alg.\ 5)_{DR}$	2.243	349	23144	0.0151

6 Conclusions

A contact enforcement algorithm has been developed for matrix-free Conjugate Gradients (CG) and Dynamic Relaxation (DR) quasistatic finite element techniques. The algorithm introduces an intermediate iteration for treating the active gap constraint and at the same time exactly (kinematically) enforces the linearized gap *rate* constraint for both frictionless and frictional response.

The essential feature of this approach is to move the normal gap constraint and tangential stick-slip constraint outside the CG (or DR) iterative solution loop. Thus, the inherently non-linear stick-slip frictional phenomenon can be robustly treated.

Furthermore, global determination of the contact constraints every iteration is no longer necessary making contact constraint definition much more efficient.

Two examples were provided to demonstrate these important aspects of the proposed algorithm.

7 References

[1] Kikuchi, N. & Oden, J.T., *Contact Problems in Elasticity: A Study of Variational Inequalities and Finite Element Methods*, SIAM, Philadelphia, 1988

[2] Heegaard, J.-H. & Curnier, A., "An augmented lagrangian method for discrete large-slip contact problems," *International Journal for Numerical Methods in Engineering*, 1993, **36** 569-593

[3] Wriggers, P., Vu Van, T. & Stein, E., "Finite element formulation of large deformation impact-contact problems with friction," *Computers and Structures*, 1990, **37** 319-331

[4] Carpenter, N.J., Taylor, R.L. & Katona, M.G., "Lagrange constraints for transient finite element surface contact." *International Journal for Numerical Methods in Engineering*, 1991, **32** 103-128

[5] Landers, J.A. & Taylor, R.L. *An Augmented lagrangian formulation for the finite element solution of contact problems*, NCEL Contract Report CR 86.008, 1986

[6] Laursen, T.A. & Simo, J.C., "A continuum-based finite element formulation for the implicit solution of multi-body, large deformation frictional contact problems," *International Journal for Numerical Methods in Engineering*, 1993, **36** 3451-3485

[7] Simo, J.C. & Laursen, T.A., "An augmented lagrangian treatment of contact problems involving friction," *Computers and Structures*, 1992, **42** 97-116

[8] Benson, D.J. & Halquist, J.O., "A single surface contact algorithm for post-buckling analysis of shell structures," *Computer Methods in Applied Mechanics and Engineering*, 1990, **78**, 141-163

[9] Belytschko, T. & Neal, M.O. "Contact-impact by the pinball algorithm with penalty and Lagrangian methods," *International Journal for Numerical Methods in Engineering*, 1991, **31** 547-572

[10] Stone, C.M., *SANTOS: A Two-Dimensional Finite Element Program for the Quasistatic Large Deformation Inelastic Response of Solids*, Report SAND90-0543, Sandia National Laboratories, Albuquerque, NM, 1990

[11] Biffle, J.H., *JAC3D - A Three-dimensional Finite Element Computer Program for the Nonlinear Quasistatic Response of Solids with the Conjugate Gradient Method*, Report SAND87-1305 UC-814, Sandia National Laboratories, Albuquerque, NM, 1993

[12] Blanford, M.L., *JAS3D - A Finite Element Computer Program* , Report SANDxx-xxxx UC-814, Sandia National Laboratories, Albuquerque, NM, 1996

[13] Shewchuck, J.R.,*An Introduction to the Conjugate Gradient Method Without the Agonizing Pain*, Available by anonymous FTP to WARP.CS.CMU.EDU (IP address 128.2.209.103) under filename `quake-papers/painless-conjugate-gradient.ps`, Carnegie Mellon University, Pittsburgh, PA, 1994

[14] Krieg, R.D. & Stone, C.M., "Methodology for Proving Contact Algorithms in Structural Analysis Codes," Proceedings 1988 Cube Symposium, Sandia National Laboratories, Albuquerque, NM, 1988

Distribution

MS0841	09100	Hommert, Paul J.
MS0443	09117	Morgan, Harold S. (40)
MS0443	09117	Heinstein, Martin W. (20)
MS0437	09118	Thomas, Robert K.
MS0321	09200	Camp, William J.
MS0439	09234	Martinez, David R.
1	MS 9018	Central Technical Files, 8940-2
5	MS 0899	Technical Library, 4916
2	MS 0619	Review & Approval Desk, 12690 For DOE/OSTI